Spectral Nonlocal Restoration of Hyperspectral Images With Low-Rank Property

Rui Zhu, Mingzhi Dong, and Jing-Hao Xue

Abstract—**Restoration is important in preprocessing hyperspectral images (HSI) to improve their visual quality and the accuracy in target detection or classification. In this paper, we propose a new low-rank spectral nonlocal approach (LRSNL) to the simultaneous removal of a mixture of different types of noises, such as Gaussian noises, salt and pepper impulse noises, and fixed-pattern noises including stripes and dead pixel lines. The low-rank (LR) property is exploited to obtain precleaned patches, which can then be better clustered in our spectral nonlocal method (SNL). The SNL method takes both spectral and spatial information into consideration to remove mixed noises as well as preserve the fine structures of images. Experiments on both synthetic and real data demonstrate that LRSNL, although simple, is an effective approach to the restoration of HSI.**

Index Terms—**Hyperspectral image, low rank (LR), nonlocal means, restoration, spectral and spatial information.**

I. INTRODUCTION

HYPERSPECTRAL images (HSI) are captured on 100s of narrow spectral bands ranging from 400 to 2400 nm, represented as a three-dimensional (3-D) data cube containing both spectral and spatial information. During the capture of HSI, various kinds of noises are introduced, polluting the images. The noises also affect further HSI applications such as classification, target detection, and unmixing. In order to recover clean images and facilitate further applications, image restoration is required as a preprocessing.

The restoration of HSI has attracted considerable attention recently [1]–[10]. The 3-D representation of HSI makes the HSI restoration different from the traditional two-dimensional (2-D) image restoration, with both spectral and spatial information at our disposal.

Common denoising methods, such as maximum noise fraction (MNF) [4], orthogonal, or oblique subspace projection [5], [6], and frequency domain filtering [7], [8], reconstruct the image in a transformed domain. They, however, fail to restore image edges effectively. Wavelet-based restoration methods [8]–[10] can preserve details of images such as edges. However, it depends on prior knowledge to choose an appropriate type of wavelet transform. Besides being represented in a transformed domain, spatial information in the original image can be exploited directly. Most of the methods that consider spatial

information are based on local information from neighbouring pixels. However, local methods exploit limited information of the true image. In contrast, nonlocal approaches use information from the whole image, based on the assumption that a small patch of the image can be represented by similar patches in other places of the same image [11]. In this way, the fine spatial structures of the image can be preserved. Qian and Ye [1] adopted this idea and applied a nonlocal sparse model to the HSI restoration, in which the overlapped patches of the image are clustered and a sparse learning method is applied to each cluster. In [1], patches in each cluster are assumed to be represented by the same dictionary. However, how to choose the dictionary is based on certain prior knowledge.

Without using prior knowledge, Golbabaee and Vandergheynst [2] and Zhang *et al.* [3] solved the HSI restoration problem utilising the low-rank (LR) property of HSI. The LR property can be attributed to the high correlation between hyperspectral signatures of pixels. Hence, the images can be expressed by a linear combination of a limited number of endmembers. In [3], an LR matrix recovery model was developed to simultaneously remove several types of noises, such as Gaussian noises, impulse noises, stripes, and dead lines. Stripes and dead lines are fixed-pattern bad pixels due to variations in detection [5], [8], [12]. Impulse noises, stripes, and dead lines can be sparse, since they only appear in few bands or few pixels within a band.

However, the LR methods, mainly exploiting the spectral correlation between spectral bands, may not preserve fine spatial structures. On the other hand, the nonlocal techniques mainly exploit the spatial correlation between spatial patches.

Hence, to exploit the best of both worlds, in this paper we propose a new low-rank spectral nonlocal (LRSNL) approach, which will consider both spectral and spatial information. It combines both the LR property of HSI and the nonlocal method for the HSI restoration. In addition, we extend the standard nonlocal approach for 2-D images to 3-D HSI, using spectral information to remove the mixed noises as well as preserve the fine spatial structures of the image.

II. METHODOLOGY

The proposed HSI restoration approach (LRSNL) contains two major parts: 1) using the LR property to obtain pre-cleaned patches and 2) applying the spectral nonlocal (SNL) method to restore the image. The LR precleaning is to improve the performance of the nonlocal restoration. The importance of precleaning has been shown in the experiments of [13] and [14], where better clustering results of the patches are obtained after a

The authors are with the Department of Statistical Science, University College London, London WC1E 6BT, U.K. (e-mail: rui.zhu.12@ucl.ac.uk; mingzhi.dong.13@ucl.ac.uk; jinghao.xue@ucl.ac.uk).

first round of denoising. We shall also demonstrate this through our experiments.

A. LR Precleaning of HSI

To explain the LR property of HSI, we first transform the 3-D data cube into a 2-D matrix. Suppose the size of an HSI data cube is $M \times N \times Q$, where M and N represent the total numbers of pixels in height and width, and Q is the number of spectral bands. The cube can be rearranged as a 2-D matrix of $(M \times N) \times Q$, with each column representing the reflectance from a specific spectral band, and each row representing the spectral signature of a specific pixel. Note that the spatial information is nevertheless lost after this transformation.

The LR property can be associated with the linear mixing model of HSI. In the linear mixing model, HSI are considered as a linear mixture of several endmembers: $\widetilde{U} = \mathbf{A}\mathbf{S}^T$, where $\widetilde{U}$ is the transformed 2-D matrix of the HSI and $\mathbf{A}$ is an $(M \times N) \times K$ matrix representing the abundance of K endmembers; the endmembers are concatenated into a $Q \times K$ matrix $\mathbf{S}$. Since there are a limited number of endmembers, the rank of $\widetilde{U}$ is limited [2].

The captured noisy HSI can be modeled as

$$\boldsymbol{V} = \boldsymbol{U} + \boldsymbol{N} \tag{1}$$

where $\boldsymbol{V}$ is the noisy HSI cube, $\boldsymbol{U}$ is the true, clean HSI cube, and $\mathbf{N}$ denotes the noise [15].

To preclean the noisy $\boldsymbol{V}$, the HSI cube is first divided into small patches of size $m \times m \times Q$, where m is much smaller than $\min(M, N)$. Each patch is centred at a pixel, thus the number of patches is $M \times N$. All the patches are transformed to 2-D matrices of size $(m \times m) \times Q$. For pixel (i, j), $i = 1, \ldots, M$ and $j = 1, \ldots, N$, its noisy patch matrix $\boldsymbol{V}_{ij}$ is precleaned by using the LR property of HSI

$$\widehat{U}_{ij} = \arg\min_{U_{ij}} \| V_{ij} - U_{ij} \|_F^2 \ \text{ s.t. } \ rank(\boldsymbol{U}_{ij}) \leq K \tag{2}$$

where $\boldsymbol{V}_{ij}$ and $\boldsymbol{U}_{ij}$ denote the noisy and clean patch matrices centred at (i, j), respectively, $\| \cdot \|_F$ denotes the Frobenius norm of matrix, and K is a predefined constant that indicates the maximal rank of the clean patch matrix [15].

As we mentioned, the LR methods only consider the spectral correlation, and thus may not preserve the fine spatial structures of the image. Fig. 1 shows the LR restoration results from LRMR [3] for two bands of a synthetic Indian Pines dataset. (The construction of this synthetic dataset will be detailed in Section III-A). We can observe that in both cases using only the LR property tends to over-smooth the images. To further recover the fine spatial structures, we propose a spectral nonlocal approach.

B. Spectral Nonlocal Restoration of HSI

The standard nonlocal means algorithm (NL) for 2-D images [11] considers the spatial information of images and aims to preserve the fine structures during image restoration. In NL, the image is divided into small patches and each pixel is restored
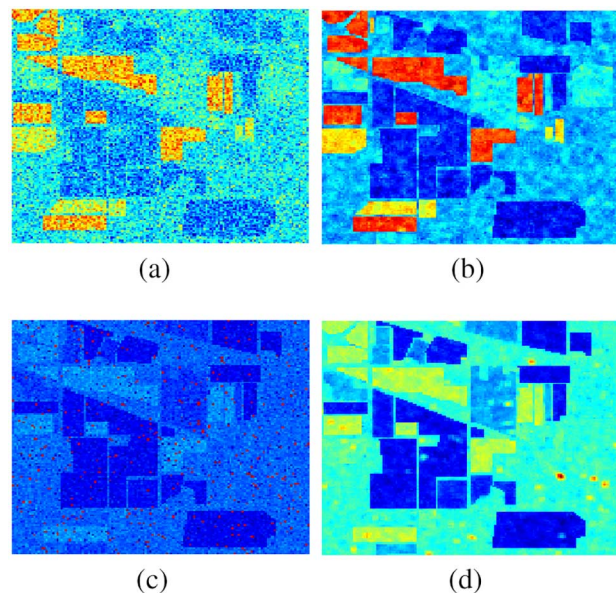

Fig. 1. LR restoration of two images: images with (a) Gaussian noises and (c) a mixture of Gaussian and impulse noises, and their LRMR results in (b) and (d), respectively.

as the weighted average of the pixels that have a neighborhood similar to the neighborhood of the target pixel. Although NL can effectively remove Gaussian noises, it cannot handle fixed-pattern noises such as dead pixel lines and stripes. For a dead pixel, the pixels that have the most similar neighbors will be the neighboring dead pixels, hence the neighboring dead pixels will have large weights and the restoration of a dead pixel is still a dead pixel.

To extend NL for HIS reconstruction, we incorporate the spectral information into NL. In our proposed method LRSNL, we assume that the weights of pixels, that have a neighborhood similar to that of the target pixel, are the same over all spectral bands. These weights are thus calculated based on the mean dissimilarity between patches over all bands. As a result, if dead lines and stripes are few, the effect of these noises will be small and the bands containing these noises can be restored by using information from other spectral bands. In this way, we extend the standard NL to a SNL, such that it can be readily applied to HIS to reduce various types of noises.

Fig. 2 illustrates the difference between NL and SNL for HIS. Fig. 2(a) shows a part of a spectral band of the Indian Pines synthetic data. The areas with the same colour have the same land cover. Fig. 2(b) shows the noisy image with two dead pixel lines, and P is a dead pixel on the left-hand line. The colour of P, different from other dead pixels, is to visually indicate its position. The true value of pixel P is 0.190 and the noisy value is 0. Fig. 2(c) and (d) shows the pixels similar to P found by NL and SNL, respectively. The dead pixels in squares A and B are the similar pixels found by NL, so clearly P will be restored as a dead pixel with value remaining 0. In contrast, the similar pixels found by SNL are all the pixels in squares C and D. Although there are dead pixels in the two squares, a large number of normal pixels will overwhelm the influence of the dead pixels. The restored value of P by using SNL is actually 0.178, close to its true value.
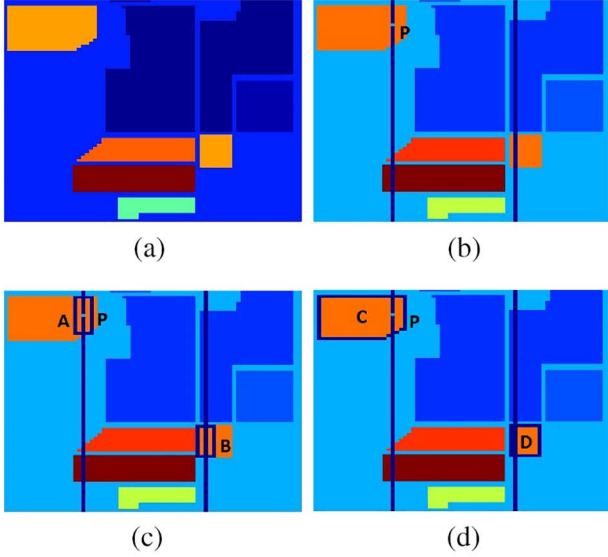
Fig. 2. Comparison of NL and SNL for dead lines: (a) original; (b) noisy; (c) NL; and (d) SNL.

Let us describe the SNL algorithm as follows. Instead of calculating the similarity between patches based on the precleaned 2-D matrix, we transform the 2-D matrix back to the 3-D cube and calculate the similarity based on this cube. The dissimilarity between two patches, respectively, centred at pixels (i, j) and (k, l), can be defined as

$$D_{ij,kl} = \frac{1}{Q} \sum_{q=1}^{Q} \| \widehat{U}_{ij,q} - \widehat{U}_{kl,q} \|_F^2, \quad k \neq i \text{ or } l \neq j \quad (3)$$

where q indexes the spectral bands. The pixel (i, j) can be recovered by a weighted average of all other pixels in the image. The weight that pixel (k, l) carries to pixel (i, j) can be expressed as

$$w_{ij,kl} = \frac{e^{-D_{ij,kl}/h^2}}{\sum_{k,l} e^{-D_{ij,kl}/h^2}} \quad (4)$$

where h is the parameter indicating the decay of the exponential function, which reduces the weight with the dissimilarity between the two patches.

From (3), we can see that the dissimilarity between two patches is evaluated as the average of the dissimilarity over all spectral bands. That is, the weights for restoring each pixel take advantage of the spectral information available. Hence, pixels affected by impulse noises or dead pixels can then be restored through using information from other spectral bands.

In NL and SNL, each patch is compared with all other patches and all the associated weights are calculated. This will result in high-computational costs when the image is large. To reduce the costs, Buades *et al.* [11] suggest to set a searching area, compute the dissimilarity between the patches within this area, and restore a pixel based on the weighted average only within this area.

Although the proposed SNL can remove mixed noises and preserve the fine structures of images, it cannot perform well

Algorithm 1. LRSNL: Low-Rank Spectral Nonlocal

Input: V, m, K, h
Output: $U^{cleaned}$
1: Divide the data cube V into overlapped patches of size $m \times m \times Q$. Transform each patch into a 2-D matrix of size $(m \times m) \times Q$.
2: Preclean patches using the low-rank property as (2).
3: Calculate the weights between the precleaned patches using (3) and (4).
4: Restore each pixel using the weighted average of all other pixels in the searching area to obtain $U^{cleaned}$.

---

when pixel values are largely affected by noises since the pixels are restored as the weighted average of pixels within the image. Using LR as a precleaning step will remove some noises and thus lead to better clustering and restoration.

Therefore, the proposed LRSNL can be summarized in Algorithm 1.

III. EXPERIMENTS

A. Synthetic Data Experiments

1) Data and Experimental Settings: An Indian Pine dataset is used for our synthetic experiments. The dataset is created based on the ground truth of Indian Pine (http://www.ehu.es/ccwintco/index.php?title=Hyperspectral_Remote_Sensing_Scenes) and the spectral signatures from the USGS digital spectral library (http://speclab.cr.usgs.gov/spectral.lib06). The ground truth describes the real land cover materials of the Indian Pine area and thus this synthetic dataset can be viewed as clean HSI that represent a real-world situation. This dataset has been widely used for validating the techniques of hyperspectral image processing and analysis [1]. The image of Indian Pine is of size 145×145 and the spectral signatures in the library describe the reflectance of 223 spectral bands. According to the ground truth, pixels of the image are classified into 17 categories. Each pixel is assigned with a spectral signature based on its category. Thus, the synthetic data cube is of size $145 \times 145 \times 223$ with reflectance values within range $[0, 0.5]$.

The performance of restoration methods is evaluated in two ways. First, the restored images and spectral signatures are shown directly for visual comparison. Since, there are numerous pixels and spectral bands, only a few of them are presented in this paper. Second, the performance is also quantitatively measured by the improved signal to noise ratio (ISNR) for each spectral band [1]

$$ISNR_i = 10 \log_{10} \frac{\sum_{x=1}^{M} \sum_{y=1}^{N} [u_i^{noised}(x,y) - u_i(x,y)]^2}{\sum_{x=1}^{M} \sum_{y=1}^{N} [u_i^{cleaned}(x,y) - u_i(x,y)]^2} \quad (5)$$

where M and N are the numbers of rows and columns of the image of a specific spectral band, $u_i^{noised}(x,y)$ is the noisy value of a pixel (x,y) of band i, $u_i(x,y)$ is its true value, and $u_i^{cleaned}(x,y)$ is its restored value.
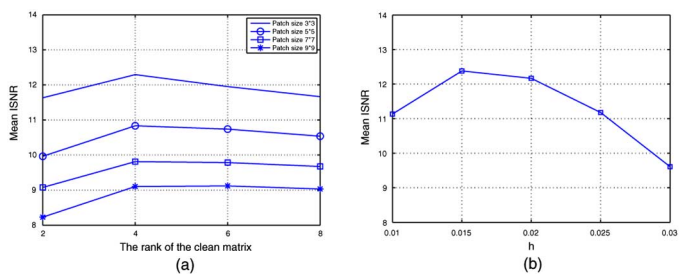
Fig. 3. Effect of tuning parameters: (a) the patch size and the rank of the clean matrix; and (b) the filtering parameter h.
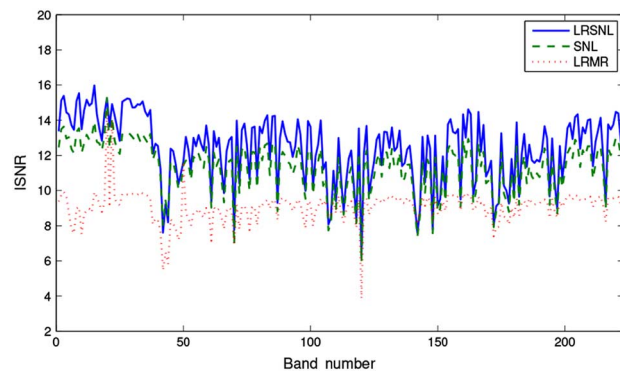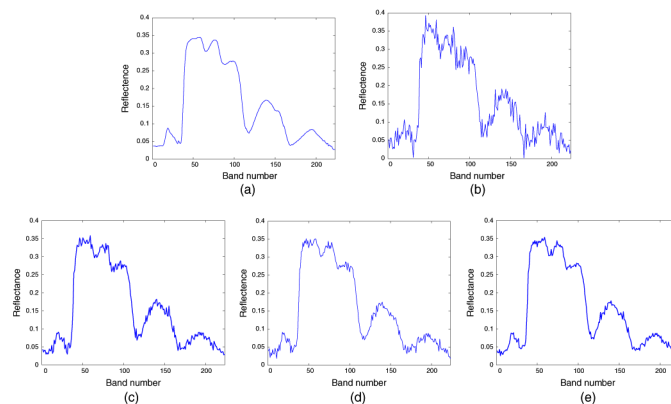

Fig. 4. ISNR of LRMR, SNL, and the proposed LRSNL.

Fig. 5. Restoration of the spectral signature of pixel $(136, 21)$: (a) original; (b) noisy; (c) LRMR; (d) SNL; and (e) LRSNL.

As with [3], our synthetic dataset covers four types of noises: 1) Gaussian noises with standard deviation ranging from 0.01 to 0.03 are added randomly to all the spectral bands; 2) 20% salt and pepper impulse noises are added to band 20 and band 22; 3) dead lines are added to band 5 to band 14 in the same positions; and (4) stripes are added to band 50 and 70. Due to the similarity between dead lines and stripes, we omit the presentation of results for stripes in this paper.

The proposed method (LRSNL) is compared with the LR matrix recovery method (LRMR) [3] and the SNL that does not have the LR precleaning step. LRMR transforms the 3-D cube into a 2-D matrix and takes advantage of the LR property of the 2-D matrix. The mixed noises are removed by using the LR matrix recovery model, which treats the clean image as a LR matrix and treats the noises, such as impulse noise and dead lines, as a sparse matrix. The GoDec algorithm [16] is used to solve the optimization problem in LRMR. We also compare LRSNL with SNL to show the effect of precleaning.

There are three parameters in Algorithm 1 to be tuned: the patch size, the rank of the clean matrix, and the filtering parameter h. The average ISNR is chosen as the performance measure. The performance of LRSNL with respect to the patch size and the rank of the clean matrix is shown in Fig. 3(a). Since the standard deviation is in the range of $[0.01, 0.03]$, h is simply set to the mean of this interval, 0.02. The performance is relatively stable when the rank is larger than 4, given the patch size. Hence, when we explore the effect of the filtering parameter h, we fix the patch size to 3×3 and the rank to 4. Fig. 3(b) plots the performance of LRSNL with respect h in this case. It shows that the value of h is slightly better to be 0.015 than 0.02. Hence, we set the value of h in (4) to 0.015.

For all methods, the 3-D cube is divided into small patches of size $3 \times 3 \times 223$, and each small patch is transformed into a 2-D matrix of size 9×223. In LRMR, the rank of the clean matrix is chosen from $\{2, 4, 6, 8\}$ and the cardinality of the sparse matrix is chosen from $\{30, 50, 70, 100\}$. The 16 combinations of the two parameters are evaluated and the best combination is chosen based on the average ISNR. The combination of rank 2 and cardinality 50 provides the best performance and is chosen for the experiments. In our LRSNL, the rank is set to 4. To reduce the computational cost, the searching area is set to a 21×21 square centred at the target pixel in the SNL step of LRSNL, by following the experiments in [11].

2) Results: Fig. 4 is the plot of ISNR versus all bands. It shows that our method can restore the noisy images better than

do LRMR and SNL in almost all spectral bands. We note that the performances of LRSNL, LRMR, and SNL at band 140 are almost the same. This is mainly because only small Gaussian noise with a standard deviation of 0.016 has been added to the band. LRMR can perform well on bands with such small Gaussian noise, but compared with LRSNL and SNL it cannot remove large mixed noises in other bands. The restored spectral signatures of pixel $(136, 21)$ are shown in Fig. 5. Compared with the original spectral signature, LRSNL also provides the best results while LRMR performs the worst.

A synthetic image with only Gaussian noises and its restored images are shown in Fig. 6. The result from LRMR shows that large Gaussian noises cannot be effectively removed, edges are over-smoothed, and fine details are lost. Compared with LRMR, SNL, and LRSNL remove most of Gaussian noises and recover the fine details of the original image. The colours of the results of LRSNL are much closer to those of the original image compared with those of SNL, which indicates that LRSNL produces an image closer to the original image.

Fig. 7 presents the restoration results of an image with a mixture of Gaussian and impulse noises. LRSNL performs the best among the three methods. Blurred white dots in Fig. 7(c) indicate that LRMR performs badly on removing impulse noises. Gaussian noises also still exist in the LRMR results. LRSNL and SNL can remove most of the impulse noises, but SNL provides a much darker image than does LRSNL.
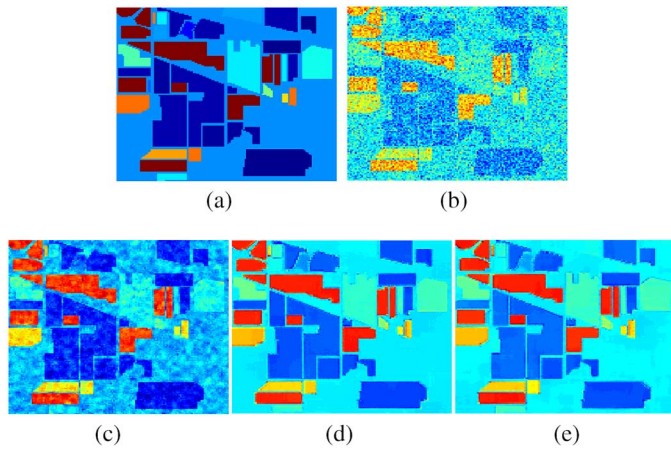
Fig. 6. Restoration of band 30 with Gaussian noises: (a) original; (b) noisy; (c) LRMR; (d) SNL; and (e) LRSNL.
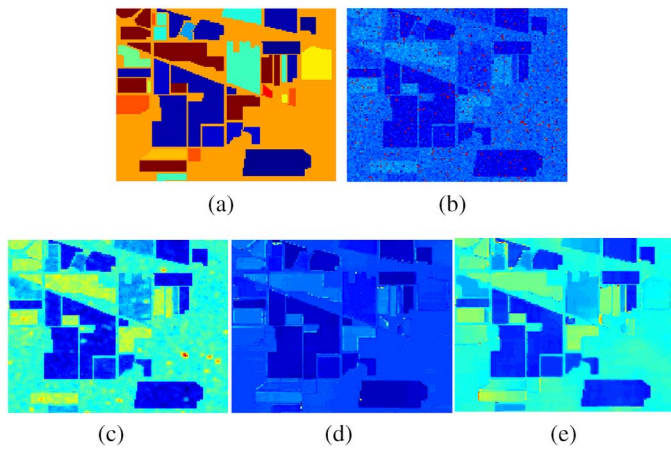

Fig. 7. Restoration of band 20 with a mixture of Gaussian and impulse noises: (a) original; (b) noisy; (c) LRMR; (d) SNL; and (e) LRSNL.
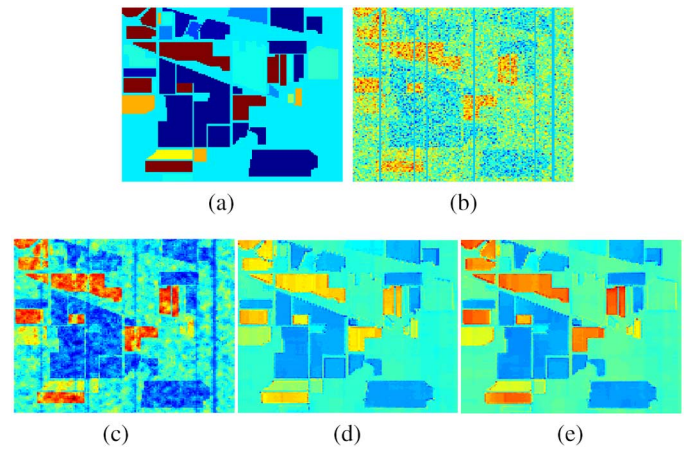

Fig. 8. Restoration of band 14 with a mixture of Gaussian noises and dead pixel lines: (a) original; (b) noisy; (c) LRMR; (d) SNL; and (e) LRSNL.
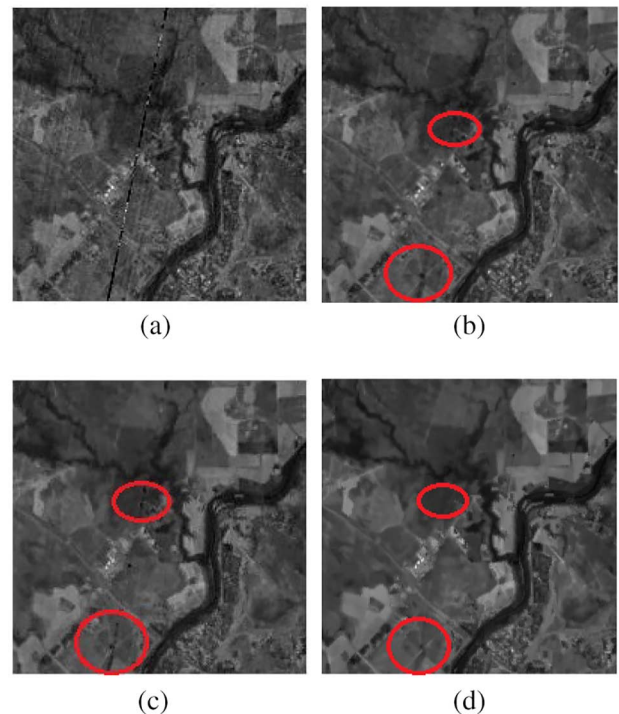

Fig. 9. Restoration of band 130 of an EO-1 Hyperion dataset: (a) original; (b) LRMR; (c) SNL; and (d) LRSNL.

Compared with LRMR and SNL, LRSNL also shows superior performance against stripes and dead pixel lines. Fig. 8 displays the restoration results of an image with a mixture of Gaussian noises and dead pixel lines, in (c) of which the blurred black lines indicate that LRMR cannot effectively remove the dead lines. Some short lines in Fig. 8(d) indicate that SNL alone cannot effectively remove the dead pixel lines that appear over several bands. Moreover, the two dead pixel lines on the right-hand side are on the edges of land covers, and Fig. 8(e) shows that LRSNL still performs well on these dead pixel lines.

In summary, from Figs. 4 to 8, we can observe that the proposed LRSNL approach performs well in all the four situations. LRMR cannot effectively remove the mixed noises, and the fine structures within the images are also lost in its restored results. SNL performs better than LRMR but worse than LRSNL, as the patches are not precleaned. The colours of the restored results confirm that the restored values of SNL are worse than those of LRSNL. SNL also cannot effectively remove the dead pixel lines that appear successively in several bands. In contrast, LRSNL can effectively remove the mixed noises as well as preserve the fine spatial structures.

B. Real-Data Experiments

An EO-1 Hyperion image dataset is used in our real-data experiments (http://eros.usgs.gov/find-data). The original dataset is of size $3371 \times 931 \times 242$. A subset of size $200 \times 200 \times 163$ is used here after the removal of water pollution bands. The pixel values of each band are normalized to $[0, 1]$ before experiments. For all methods, the dataset is first divided into patches of size $3 \times 3 \times 163$ and transformed into a 2-D matrix of size 9×163. As with the experiments in Section III-A, for LRMR, the rank of the clean image is set to 2 and the cardinality of the sparse matrix is set to 50. For LRSNL, the rank is set to 4 and the parameter h is set to 0.015. The

searching area is set to a 21×21 square centred at the target pixel.

A large number of spectral bands of the original hyperspectral data cube are polluted by a mixture of dead pixel lines, stripes, and other noises. The restoration results of band 130 are shown in Fig. 9. LRMR can only remove part of dead pixel lines and stripes, as shown in Fig. 9(b). It also tends to over-smooth some edges. Although SNL preserves more fine structures compared with LRMR, the dead pixel line still can be spotted as shown in Fig. 9(c). Apparently, LRSNL performs the best among the three methods. It can remove almost all the noises and preserve the details as well, as shown in Fig. 9(d).

IV. CONCLUSION

In this paper, we have proposed LRSNL, a simple and effective restoration method for hyperspectral images. In LRSNL, the standard NL algorithm is extended to SNL to take advantage of both spectral and spatial information. Hence, a mixture of different types of noises can be removed simultaneously, and at the same time the fine details and local structures of the clean image can be preserved. For a better clustering of the patches in SNL, the LR property of the clean hyperspectral image is exploited in a precleaning step. The experiments have demonstrated the effectiveness of LRSNL and the importance of the precleaning step.

LRSNL treats all spectral bands the same and simply uses the average of all the bands to calculate similarities between patches. However, when spectral bands are of different importance, an adaptive weighting scheme is better to be developed.

ACKNOWLEDGMENT

REFERENCES

[1] Y. Qian and M. Ye, "Hyperspectral imagery restoration using nonlocal spectral–spatial structured sparse representation with noise estimation," *IEEE J. Sel. Topics Appl. Earth Observ. Remote Sens.*, vol. 6, no. 2, pp. 499–515, Apr. 2013.

[2] M. Golbabaee and P. Vandergheynst, "Hyperspectral image compressed sensing via low-rank and joint-sparse matrix recovery," in *Proc. IEEE Int. Conf. Acoust. Speech Signal Process. (ICASSP)*, 2012, pp. 2741–2744.

[3] H. Zhang, W. He, L. Zhang, H. Shen, and Q. Yuan, "Hyperspectral image restoration using low-rank matrix recovery," *IEEE Trans. Geosci. Remote Sens.*, vol. 52, no. 8, pp. 4729–4743, Aug. 2014.

[4] A. A. Green, M. Berman, P. Switzer, and M. D. Craig, "A transformation for ordering multispectral data in terms of image quality with implications for noise removal," *IEEE Trans. Geosci. Remote Sens.*, vol. 26, no. 1, pp. 65–74, Jan. 1988.

[5] N. Acito, M. Diani, and G. Corsini, "Subspace-based striping noise reduction in hyperspectral images," *IEEE Trans. Geosci. Remote Sens.*, vol. 49, no. 4, pp. 1325–1342, Apr. 2011.

[6] Q. Wang, L. Zhang, Q. Tong, and F. Zhang, "Hyperspectral imagery denoising based on oblique subspace projection," *IEEE J. Sel. Topics Appl. Earth Observ. Remote Sens.*, vol. 7, no. 6, pp. 2468–2480, Jun. 2014.

[7] J. G. Liu and G. L. K. Morgan, "FFT selective and adaptive filtering for removal of systematic noise in ETM+ imageodesy images," *IEEE Trans. Geosci. Remote Sens.*, vol. 44, no. 12, pp. 3716–3724, Dec. 2006.

[8] R. Pande-Chhetri and A. Abd-Elrahman, "De-striping hyperspectral imagery using wavelet transform and adaptive frequency domain filtering," *ISPRS J. Photogramm. Remote Sens.*, vol. 66, no. 5, pp. 620–636, 2011.

[9] A. Duijster, P. Scheunders, and S. De Backer, "Wavelet-based EM algorithm for multispectral-image restoration," *IEEE Trans. Geosci. Remote Sens.*, vol. 47, no. 11, pp. 3892–3898, Nov. 2009.

[10] B. Rasti, J. Sveinsson, M. Ulfarsson, and J. Benediktsson, "Hyperspectral image denoising using first order spectral roughness penalty in wavelet domain," *IEEE J. Sel. Topics Appl. Earth Observ. Remote Sens.*, vol. 7, no. 6, pp. 2458–2467, Jun. 2014.

[11] A. Buades, B. Coll, and J.-M. Morel, "A review of image denoising algorithms, with a new one," *Multiscale Model. Simul.*, vol. 4, no. 2, pp. 490–530, 2005.

[12] Q. Li, H. Li, Z. Lu, Q. Lu, and W. Li, "Denoising of hyperspectral images employing two-phase matrix decomposition," *IEEE J. Sel. Topics Appl. Earth Observ. Remote Sens.*, vol. 7, no. 9, pp. 3742–3754, 2014.

[13] J. Mairal, F. Bach, J. Ponce, G. Sapiro, and A. Zisserman, "Non-local sparse models for image restoration," in *Proc. IEEE 12th Int. Conf. Comput. Vis. (ICCV)*, 2009, pp. 2272–2279.

[14] K. Dabov, A. Foi, V. Katkovnik, and K. Egiazarian, "Image denoising by sparse 3-D transform-domain collaborative filtering," *IEEE Trans. Image Process.*, vol. 16, no. 8, pp. 2080–2095, Aug. 2007.

[15] X. Zhou and W. Yu, "Low-rank modeling and its applications in medical image analysis," in *Proc. SPIE Defense Secur. Sens.*, 2013, p. 87500V.

[16] T. Zhou and D. Tao, "GoDec: Randomized low-rank and sparse matrix decomposition in noisy case," in *Proc. 28th Int. Conf. Mach. Learn. (ICML)*, 2011, pp. 33–40.

Rui Zhu received the B.S. degree in engineering from Xiamen University, Xiamen, China, in 2012, and the M.Sc. degree in statistics from the University College London, London, U.K., in 2013. She is currently pursuing the Ph.D. degree at the Department of statistical science, University College London.

Her research interests include spectral data analysis, hyperspectral image analysis, and metric learning.
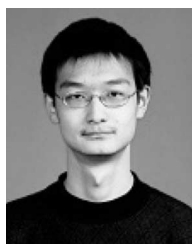
Mingzhi Dong received the B.Eng. degree in automation, and the M.Eng. degree in signal and information processing from Beijing University of Posts and Telecommunications, Beijing, China, in 2010 and 2013, respectively.

He is currently a Research Student with the Department of Statistical Science, University College London, London, U.K. His research interests include data analysis, pattern recognition, and machine learning.

Jing-Hao Xue received the Dr. Eng. degree in signal and information processing from Tsinghua University, Beijing, China, in 1998, and the Ph.D. degree in statistics from the University of Glasgow, Glasgow, U.K., in 2008.

Since 2008, he has been with the Department of Statistical Science, University College London, London, U.K., as a Lecturer and Senior Lecturer. His research interests include statistical classification, high-dimensional data analysis, computer vision, and pattern recognition.